Transient stratified corium pool modelling for In-Vessel Retention analysis

Romain Le Tellier, Louis Viot, Laure Carénini, Florian Fichot, Nikolai Bakouta, Aleksandr Filippov

International Seminar "In-vessel retention: outcomes of IVMR project"
Palais des Congrès, Juan-les-Pins, France, January 21-22, 2020

Transient stratified corium pool modelling for In-Vessel Retention analysis

R. Le Tellier[1], L. Viot[1], L. Carénini[2], F. Fichot[2], N. Bakouta[3], A. Filippov[4]
[1]: CEA, DEN, DTN/SMTA/LMAG, Cadarache – 13108 Saint Paul-lez-Durance, FRANCE
[2]: IRSN, BP3 – 13115 St Paul lez Durance, FRANCE
[3]: EDF, EDF Lab, Paris-Saclay, 7 boulevard Gaspard Monge, 91120 Palaiseau, FRANCE
[4]: IBRAE, 52 B. Tulskaya St. Moscow, RUSSIA

romain.le-tellier@cea.fr, louis.viot@cea.fr, laure.carenini@irsn.fr, florian.fichot@irsn.fr, nikolai.bakouta@edf.fr, phil@ibrae.ac.ru

Abstract

Considering the in-vessel-retention strategy for the management of severe accident in light water reactors, this paper provides an overview of state-of-the-art modelling under transient conditions of the core melt behaviour in the lower head. This presentation is based on a cross-comparison between the models of four different codes, namely, ASTEC (IRSN), HEFEST (IBRAE), EDF proprietary version of MAAP5 (EPRI) and PROCOR (CEA) and is illustrated by some results from a recent benchmark exercise carried out in the frame of the European IVMR project. Apart from pool thermal-hydraulics and vessel wall ablation, some emphasis is put on melt thermochemistry and transient phase segregation (boundary crust formation/disappearance and liquid phase stratification). As highlighted in the benchmark exercise, the main associated uncertainties in terms of heat flux at the vessel wall external boundary are related to the stratification transients and the stability of the crusts in contact with light metal layer during stratification inversion transient.

Keywords: IVR, stratified corium pool modelling, pool thermal-hydraulics, corium thermochemistry, code benchmark

1. Introduction

In the frame of Severe Accident (SA) analysis for Light Water Reactors (LWR), one important topic is related to the behaviour of molten materials (aka corium) associated with the partial oxidation and possible melting of clads and fuel pellets after a loss of core cooling. More particularly, when considering the In-Vessel Retention (IVR) strategy (Henry and Fauske, 1993; Tuomisto and Theofanous, 1994) where the corium is to be maintained within the Reactor Pressure Vessel (RPV) by reflooding the reactor pit (External Reactor Vessel Cooling - ERVC), it is the corium pool relocated from the core in the RPV lower head that is of prime interest. Indeed, the thermomechanical integrity of the RPV lower head is fully dependent on the corium pool behaviour and the heat fluxes it imposes on the vessel wall.
In-vessel corium is a complex multicomponent system in terms of possible phase segregation processes including liquid phase stratification and solidification at the cooled boundaries. This complexity is related to the fact that, during the late in-vessel phase of an SA transient, in addition to fuel and clads materials (mainly, $(U_y,Zr_{1-y})O_{2-x}$), corium will be progressively enriched in molten steel elements (mainly, Fe, Ni, Cr) from the ablated internal structures and vessel wall. Since the first evaluations performed in the nineties and the associated model developments, progresses in the understanding of the thermochemistry of the corium in the lower head when mixed with molten steel were made, mainly thanks to the results of the OECD MASCA 1 and 2 programs (Tsurikov et al. 2007). It was found in particular that the chemical interactions in the melt pool have a direct impact on its stratification and need to be considered in the evaluations of IVR strategy (Tuomisto and Sehgal, 2007).

Because of this strong coupling between thermal-hydraulics and thermochemical phenomena in the pool, the heat and mass exchanges between the melt and the steel structures, the thermal load to the vessel wall and its ablation

have to be evaluated under transient conditions. This requirement was made very clear in the course of the European H2020 project IVMR (In-Vessel Melt Retention) that aimed at revisiting the SA strategy of IVR, in particular for ''high-power"[1] reactor *(i.e.* 1000 MWe or more) (Fichot et al. 2018; M. Sangiorgi et al. this seminar). In this framework, modelling (and the associated validation) is made more difficult in comparison with earlier stationary models involved in bounding case simulations (Esmaili and Khatib-Rahbar, 2004).

In this paper, salient aspects of this transient modelling (excluding the formation of the pool involving e.g. solid debris melting) are discussed through the lens of the models in the ASTEC, HEFEST, EDF proprietary version of MAAP5 referred as MAAP_EDF and PROCOR codes that were used and compared in the frame of a benchmark exercise carried out during the IVMR project (Carénini et al. 2019). The key issues associated with stratified pool modelling and their impacts on the heat flux imposed to the vessel wall are highlighted.
First, Section 2 gives an overview of the stratification phenomenology as characterized in past experiments and more recent ones carried out in the frame of the IVMR project. Then, modelling in the different codes is discussed in Sections 3 and 4. While Section 3 gives an overview of thermal-hydraulics modelling and highlights important modelling features regarding heat transfer from the pool to its surroundings, Section 4 is focused on melt thermochemistry, mass-transfer and transient phase spatial distribution.

2. Overview of stratification phenomenology and associated knowledge

Considering the U-O-Zr-Fe(-Ni-Cr) system to be representative of in-vessel corium composition and thermodynamics, past experimental programs on suboxidized corium-steel interactions (in particular, OECD MASCA 1 and 2) have shown that the miscibility gap exhibited at liquid state leads, at steady-state, to melt component partitioning into an oxygen-rich ("oxide") phase and an oxygen-poor ("metal") phase. When their density difference is large enough, these two phases tends to stratify into a two-layer pool. For a low Zr oxidation degree C_{Zr} or steel mass fraction x_{steel}, the "metal" phase density is higher than the oxide one (because of a relatively large mass fraction of Uranium) and tends to decrease when C_{Zr} or x_{steel} increases.

During an SA transient where C_{Zr} and x_{steel} are both likely to increase, the stratification can be modified according to two possible transients illustrated schematically in Figure 1 (a) where a transient 3-layer configuration is depicted. Because of the small scale (≤ 2kg of corium) of all-but-one MASCA experiments, the transient kinetics is not characterized. Only the MASCA-RCW test where 5kg of molten steel were poured on top of about 45kg of suboxidized corium for a 22' exposure time can be related to the heavy metal layer formation transient by the analysis of the solidified ingot (see Figure 1 (b)). Qualitatively, the phenomenology associated with this experiment can be described by the following steps:

- interfacial mass transfer of U, Zr from the oxide to the steel leads to a high-density metal boundary layer;
- Rayleigh-Taylor (R-T) instabilities develop at the interface in such a way that metal droplets detach and sink into the oxide;
- droplets coalescence leads to a continuous heavy metal phase at the bottom of the pool.

Interfacial mass transfer with a characteristic time of 1000s appears as the limiting kinetic factor (in comparison with droplets hydrodynamics) and the overall metal relocation process is likely to be intermittent (Ratel et al. 2007).

In MASCA program experiments, no stable crust at the metal/oxide interface was present and it was argued in some publications (see for instance, (Gu et al. 2013)) that such a crust could be mechanically stable in the reactor case and prevent the interaction between suboxidized corium and steel. Series 1 of the CORDEB program (Almjashev et al. 2018) and, subsequently, the CORDEB2 program (in the frame of the IVMR project) were focused on the impact of a stable crust on the pool stratification. It was shown that:

- crust dissolution by molten steel makes the crust permeable in such a way that it does not prevent steel interaction with corium;

[1] Here, it is the decay heat power, not the nominal power that is concerned.

- the characteristic time of the overall kinetics may be strongly increased by the crust presence.[2]

The analytical VITI-CORMET experiments (Pivano et al. 2019) focused on the dissolution process under isothermal conditions were carried out to supplement CORDEB2 program (Almjashev et al. this seminar). As depicted in Figure 2, it was observed in both programs that the crust dissolution is associated with the formation (during an incubation period) and growth of metal channels inside the crust in which metallic components are transported with steel components (resp. U, Zr) moving downwards (upwards). The two first-order parameters that control this process are the Zr oxidation degree of the sub-oxidized corium and the temperature of the molten steel: a large oxidation index (e.g. C_{Zr}=70%) or a reduced temperature (e.g. 1500°C) can limit percolation channel formation (with a close-to-zero limit in the fully oxidized case). At high-enough temperature (e.g. 1900°C for C_{Zr}=30%), the steady-state is likely be a two-liquid pool as would be the case in the absence of crust.

Another *a priori* important phenomenon is the pool oxidation by the gaseous atmosphere as the thermochemical equilibrium depends on the oxygen content. Different experimental programs (including MASCA) were analysed in (Almjashev et al. 2016). In all cases, the overall kinetics was found to be driven by the oxidant transport to the reactive interface (so-called oxidant starvation regime) either associated with oxygen diffusion through the crust[3] or convection in the gaseous phase in absence of crust. In (Carénini et al. 2018), by extrapolating the measured consumption rates of steam in such experiments to the reactor case, it was concluded that the oxidation rate is too low to have significant effects during the first stages of the stratified pool evolution and it will not further be discussed in this paper.

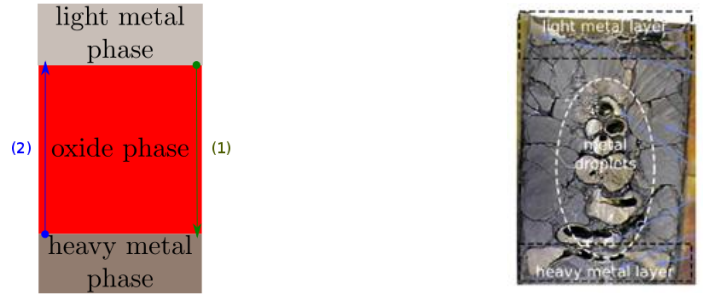

(a) Schematics of liquid phase stratification and possible transients : heavy metal layer formation (1) or disappearance (2)

(b) Cut of the solidified ingot of the MASCA-RCW experiment (adapted from (Tsurikov, 2007))

Figure 1: Illustrations of in-vessel corium stratification transients

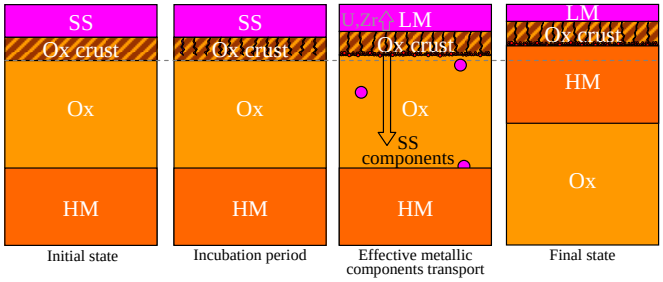

Figure 2: Schematics of molten steel-corium interaction in presence of an oxide crust as observed in the CORDEB Series 1 (adapted from program (Almjashev et al. 2018)) - SS=stainless steel, Ox=Oxide, HM=Heavy metal, LM=Light metal

[2] In the MASCA-MA6 experiment (without crust) the steady-state two-layer configuration was reached in less than half an hour while in the CORDEB-CD1 experiments (with crust and an element inventory close to MASCA-MA6), stopped after 3h, the steel mass transfer was still ongoing.

[3] These results were completed by the series 2 and 3 of CORDEB program regarding the oxidation kinetics in presence of a crust.

3. Thermal-hydraulics modelling of the stratified pool and heat transfer to its surroundings

Salient aspects of the in-vessel corium transient modelling will now be discussed through the lens of the modelling offered in:

- the lower plenum module of the ASTEC (Accident Source Term Evaluation Code) software system (Chatelard et al. 2014) ;
- the HEFEST code, a part of the HEFEST-URAN package (Filippov et al. 2014) along with HEFEST_M (thermomechanics of the ablated vessel wall based on 2D finite elements - FE) and VARIA (managing the uncertainty analysis procedure);
- the EDF's lower plenum model developed within MAAP5 computer code (Fauske & Associates Inc, 2008) licenced by EPRI;
- PROCOR-FDC application based on the PROCOR software platform (Le Tellier et al. 2015a).

The modelling scope for in-vessel corium and covered by the four codes encompasses:

- melt relocation from the core to the lower plenum;
- if some water is present inside the lower plenum, quenching and partial or total fragmentation of the slumping corium depending on corium flow rate and water availability;
- solid debris heating and secondary melting;
- corium pool formation;
- melt-structures interactions resulting in a progressive melting of steel structures;
- melt-RPV wall interactions resulting in the ablation and penetration with melt-through of the wall;
- molten material relocation (debris, internal structures and vessel wall) within the lower plenum (see Figure 3 (a) where the different mass flow rates to the pool are illustrated in the case of the ASTEC lower plenum model);
- melt phase segregation including liquid phase stratification and boundary solidification;
- thermal-hydraulics behaviour of the melt including natural convection in the liquid phases, conduction in the solid crust and radiative heat transfer at the upper boundary.

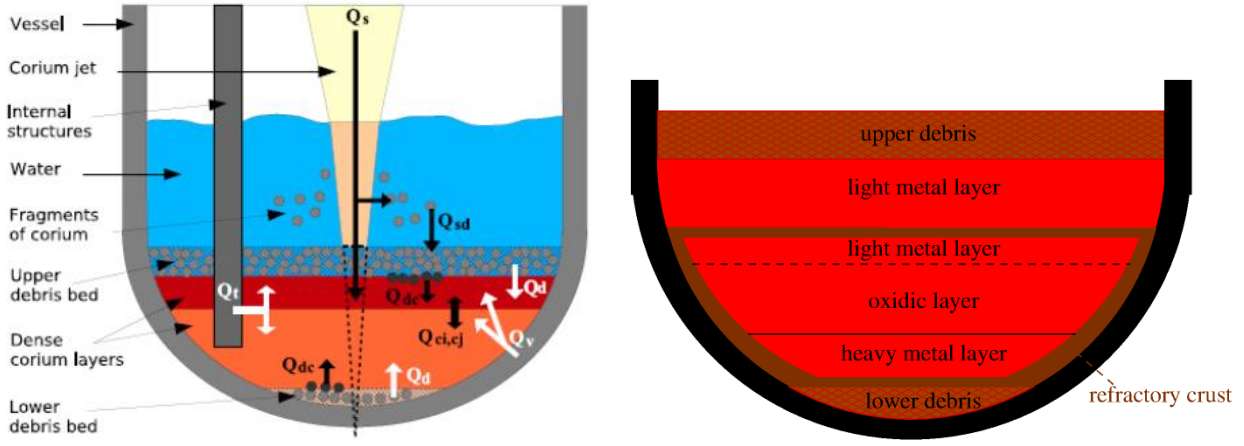

(a) Schematics of mass transfers in the lower head: example of ASTEC lower plenum model

(b) Possible stratified layers of debris and dense corium (the light metal layer below the oxidic crust is not considered in ASTEC)

Figure 3: Possible layers and components considered in the integral modelling of the ASTEC, MAAP_EDF and PROCOR codes.

In this section, we will focus on the thermal-hydraulics modelling of the stratified pool, heat transfer to the vessel wall and associated relocation of the molten steel to the pool. These are the code features (in addition to melt thermochemistry models discussed in §4) that were covered by the IVMR project benchmark exercise reported in (Carénini et al. 2019).

3.1 Pool thermal-hydraulics modelling

Regarding pool thermal hydraulics modelling, some difference exists between the HEFEST code and the three others. While HEFEST uses a 2D FE formalism to solve the transient heat conduction over the whole lower head and corium pool, ASTEC, MAAP_EDF and PROCOR are based on an integral formulation (so-called 0D modelling) of the mass and energy conservation equations for pre-determined stratified layers as depicted in Figure 3 (b).
As a consequence, while ASTEC, MAAP_EDF and PROCOR make direct use of Nusselt correlations to evaluate the heat transfer coefficient at the different boundaries of the layers, convective heat transfer is estimated in HEFEST through the effective heat conductivity method (in the bulk of fluid and/or on boundary finite elements).
Regarding the correlations, they are expressed in terms of internal (resp. external) Rayleigh number when convection is associated with the volumetric heating by the fission products (FPs) decay heat (resp. the temperature difference between adjacent corium layers - Rayleigh-Benard configuration, typically for the light metal layer - or between a layer and the vessel wall). The "best estimate" correlations used in the three codes for the oxidic and light metal layer are given in Table 1. At the interface with the inclined vessel wall, specific shape factor that depends on the vessel geometry and/or the layer under consideration are also used in order to evaluate the local heat flux at the interface. In addition, in MAAP_EDF and PROCOR, specific treatments have been implemented for the energy balance of a "thin" (typically below 20cm-height) light metal layer in direct contact with the vessel wall (the light metal layer on top of the refractory crust in Figure 3 (a)). Indeed, for such thin layers, an overestimation of the "focusing effect" (lateral flux concentration) was observed when standard correlations (that do not take into account the coupling between the axial and lateral heat transfer) are used. In MAAP5, an eddy diffusivity model is used and imposes an additional resistance which reduces the heat flux to the vessel while, in PROCOR, based on Direct Numerical Simulations of the metal layer thermal-hydraulics carried out in the frame of the IVMR project (Peybernes at al. 2020), updated correlations involving the Stefan numbers associated with radiative heat transfer at the top boundary are now available. In both cases, as illustrated in Figure 4, with such updated models, the heat flux to the reactor vessel wall decreases as the thickness of the light metal layer falls below a threshold around 5 cm.
With the effective heat conductivity method in HEFEST, interlayer heat transfer is represented by an effective heat source while side heat flux profile (including focusing effect) may be modelled through orthotropic heat conductivity or direct implementation of experimental data (FAS model) ; see (Filippov et al. 2013). Under transient conditions, this approach is limited in HEFEST to two-layer pool configurations while three-layer (or more) melt can be considered only in steady-state configuration, without evolution, as a separate effect. Simplistically, light metal layer in the unsteady tri-layer melt may be also treated as a kind of heat resistance on the upper boundary of the oxide layer.

Table 1: Correlations for the oxide and light metal layers as used in the ASTEC, MAAP_EDF and PROCOR codes

	Oxide layer	Light metal layer
Upward	$0.381.Ra_i^{0.234}$ Bonnet-Seiler's correlation (1999)	$0.17.Ra_e^{1/3}.Pr^{0.074}$ Globe-Dropkin's correlation (1959) written for half the layer height
Downward	$1.389.Ra_i^{0.095}$ Jahn's correlation (1974)	
Lateral	$0.131.Ra_i^{0.25}.\left(\frac{L}{r}\right)^{0.19}$ Bonnet-Seiler's correlation (1999)	$\frac{0.15.Ra_e^{1/3}}{\left(1+\left(\frac{0.492}{Pr}\right)^{9/16}\right)^{16/27}}$ Chawla-Chan's correlations (1982) (*)

Where:
- Ra_i is the internal Rayleigh number (volumetrically heated fluid),
- Ra_e is the external Rayleigh number (Rayleigh-Benard configuration);
- Pr is the Prandtl number ;
- L/r is a shape factor for the corium layer.

N.B. for the heavy metal layer, the configuration is different from the light metal one: it is volumetrically heated and, at the same time heated from above, cooled laterally. In this case, the different codes implement different correlations but the overall impact is limited.

(*) formulation for turbulent regime

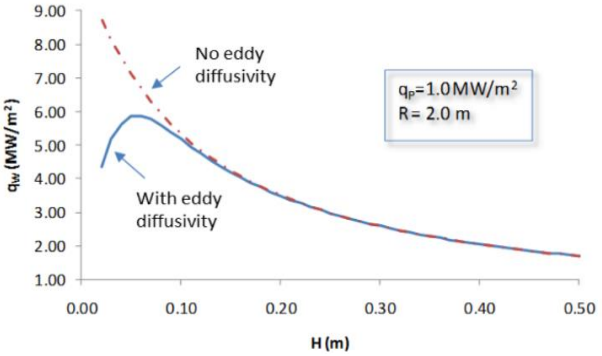

(a) Illustration of: comparison of the heat flux from the metal layer to the vessel wall with (solid line) and without (dashed line) the eddy diffusivity model used in MAAP5.

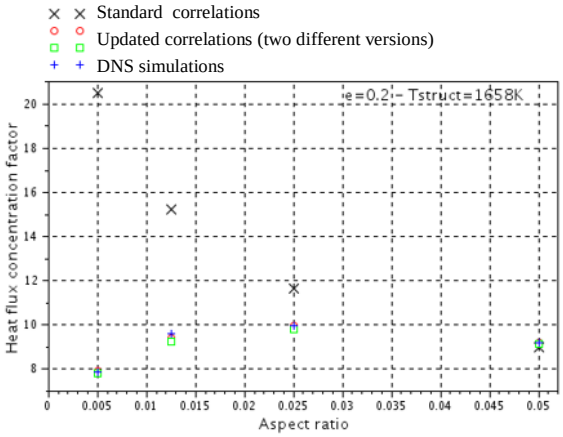

(b) Comparison of standard and updated correlations (from DNS calculations) used in PROCOR in terms of the heat flux concentration factor (ratio between lateral and bottom heat fluxes)

Figure 4: Illustrations of improved thermal modelling for thin metallic layers in MAAP_EDF and PROCOR

3.2 Radiative heat transfer at the top boundary

At the top of the pool, radiative heat transfer to upper structures is modelled.
In ASTEC and HEFEST, a model for radiative heat transfers in large cavity (assuming transparent gas) is available to consider the geometry above the pool which may differ depending on the history of the accident progression and on the reactor design. It is based on view factors between surfaces, with a possible partial or complete shading effect of some surfaces. Alternatively, in HEFEST, radiative heat transfer can be treated by a diffusion approach for optically thick medium.
In MAAP5 and PROCOR, a cruder model is applied where radiative heat flux is calculated assuming heat transfer between two parallel planes (one being the light metal layer surface).

3.3 Boundary crust treatment

Another important difference among the four codes is the treatment associated with the refractory crust that can be present at the interface between some of the pool phases and the vessel wall (referred as the "lateral crust") and the one at the bottom of the light metal layer responsible for the focusing effect (referred as the "axial crust"). In HEFEST, this crust is treated seamlessly, in frame of solution of the heat conduction equation with discontinuous coefficients. The meshing near the vessel wall inner surface is taken fine enough so that the lateral crust region (solid melt near the vessel having its own properties) contains 1-3 finite elements. This region moves with the ablation boundary. Crust composition is considered to be the same as for the oxide melt. Composition evolves during ablation in accordance with the corresponding model based on MASCA results. Solidification-melting is based on Stefan-like model but using an effective capacitance that fully takes into account the enthalpy-temperature dependency. For mixtures, the enthalpy-temperature relation is calculated by interpolation on the melt components; component heat capacities are considered as piecewise-linear functions. As for potential interlayer crust, the meshing is usually too coarse to apply the same treatment as for the lateral crust (it would lead to an unrealistically thick crust) and the heat transfer through the crust is modelled via the source term in the metallic layer as mentioned above (the source is estimated through heat flux taken from experimental data). To

minimize the "parasitic" heat transfer from the oxide layer, heat conduction in the intermediate region (2 elements) is taken small. An alternative approach (under implementation) consists in using 0D models for the melt layers heat transfer and crust properties (superimposed on the 2D mesh as a one-cell crust); this approach is close to the one described below for MAAP_EDF and PROCOR (version 2.4) codes.
In ASTEC and PROCOR (for version 2.3 and below), crusts are not modelled explicitly but considered as thermal resistances. Thus, the inertia of the crusts, their residual power and possible chemical interactions with the material they are in contact with are neglected. Such a "fictitious" crust treatment is used in MAAP_EDF and PROCOR version 2.4 but only for the axial crust. A consequence of this modelling is that the lateral oxide crust adapts instantaneously when boundary conditions change (e.g. variation of oxide pool height). In PROCOR, this crust is considered around the pool composed of the heavy metal layer, the oxide layer and, possibly, a light metal layer (see Figure 3 (a)) while, in ASTEC, such a crust is only present around the oxide pool.
During the stratification inversion transient (when light metal droplets rise to the top of the oxide pool), such a simplified approach cannot represent possible transient stages (associated with the evolution of the pool layer heights) where the lateral boundary of the light metal layer is inhomogeneous with an oxide crust in the lower part and a direct contact with the vessel wall above.
As a consequence, in MAAP_EDF and PROCOR (version 2.4), the lateral crust can be explicitly represented through an axial 1D meshing. Axial conduction in the crust is neglected and an integral conservation equations formulation is considered for each mesh with heat fluxes closures based on a quadratic temperature profile assumption (Le Tellier et al. 2017). As introduced in PROCOR in the frame of the IVMR project, for each crust mesh, depending on its composition and the composition of the melt layer in front of it, different interface conditions are considered in such a way that oxide pool solidification (Stefan condition), refractory crust fusion (Stefan condition) but also the motionless interface between a metal layer and an oxide crust (heat flux continuity) can be correctly taken into account. In MAAP_EDF, a same approach has been subsequently followed with the additional simplification that the crust composition is considered to be the same as the one of the oxide layer at any time.

Apart from its direct impact on the mass and energy balance, the crust can also play a role as a physical barrier preventing the direct (non-diffusive) mass transfer (e.g. from the partially molten vessel wall) that will be discussed in the next paragraph for the lateral crust and in § 4 along with stratification kinetics models for the axial crust.

3.4 RPV wall ablation and molten steel relocation

Regarding the RPV wall, its heating and ablation (Stefan condition) is treated by 2D meshing in ASTEC, MAAP_EDF and HEFEST and an axial 1D meshing in PROCOR. In PROCOR, as for the crust model, an integral conservation equations formulation is considered for each mesh and the axial conduction is neglected or only crudely approximated. An important difference between the codes is also associated with the relocation of vessel wall molten steel to the pool. The uncertainty associated with it is large because of crust thermo-mechanics in particular[4] and, accordingly, different hypotheses have been made in the different codes. Three different assumptions can be distinguished:

- considering that a possible interface crust is fully permeable, molten metal from a vessel mesh is incorporated into the melt at the same axial location ; this is the only option in ASTEC and a possible option in MAAP_EDF;
- considering crust non-permeability, molten metal is incorporated into the light metal layer ; this is the only option in HEFEST (each component of the arriving melt is distributed in accordance with the current stratification state) and a possible option in MAAP_EDF and PROCOR;
- an intermediate option (controlled by user parameters) is available in PROCOR : part of the molten steel is incorporated on top of the pool and the rest is considered to enter the pool and rise through it to form a light metal layer below the axial crust.

[4] Considering the thickness of the crust in the top part of the oxide pool (below 5 mm for typical heat flux of 1MW/m²), it may be postulated that it is fragmented and cannot prevent species transfers through it.

3.5 Some illustrative results

In order to illustrate the modelling features that have been presented above and the impact of their differences among the four codes, some results of the benchmark case n°3 in (Carénini et al. 2019) are now discussed. In this benchmark case where melt thermochemistry and associated transient evolution of the stratification were not considered, transient simulations were carried out starting from a prescribed two-layer pool (oxide below light metal) considering a progressive incorporation of steel due to the melting of the internal structures in the vessel and evaluating the vessel wall ablation till reaching a stabilized situation. For the sake of comparison between codes and to focus on the corium pool behaviour, the kinetics of molten steel addition from the internal structures in the corium pool is prescribed; only the vessel ablation and the pool thermal-hydraulics are simulated. The calculated heat flux profiles at the outer surface of the vessel, both at the time when the maximum value is reached (a) and at steady-state (b) are reported at Figure 1.

For all codes, the maximum value is reached before the beginning of the prescribed molten steel addition. It is evaluated in front of the top metal layer whose thickness is about 50cm (including molten steel from vessel ablation. Values are in the range 0.55-0.85MW/m². It appears that the lowest value is associated to the strong radiative heat flux evaluated in this case in MAAP_EDF code, and mainly linked to the values of the metal layer properties (high emissivity and high melting temperature in particular calculated by the code).

It is worth noting that, in HEFEST simulation, the modelling of the axial oxide crust (and the reduced conductivity of the two-element interlayer, see §3.3) limits the heat flux and hence, the vessel ablation at its location (at about 1.4m).

The melting of the vessel wall happens mainly at the beginning of the transient and leads to addition of about 10-15t of steel into the metal layer, except for the MAAP_EDF simulation in which the mass of molten steel added in the top layer from the vessel ablation is limited to 3t. This is of course directly linked with the evaluation of a smaller heat flux applied to the vessel wall in front of the metal layer due to larger dissipation by radiation. In ASTEC (resp. MAAP_EDF) simulation, assuming that the lateral crust is permeable, 7t (resp. 4.7t) of molten steel from the vessel wall are incorporated into the oxide pool (remain in this layer since thermochemical models are disabled in this case).

At steady-state because of the the simplified meshing of the vessel wall used in PROCOR[5], the "spreading" of the heat flux above the metal layer and the peaking of the flux in front of this layer (observed in ASTEC and HEFEST results) are not reproduced, see Figure 5 (b).

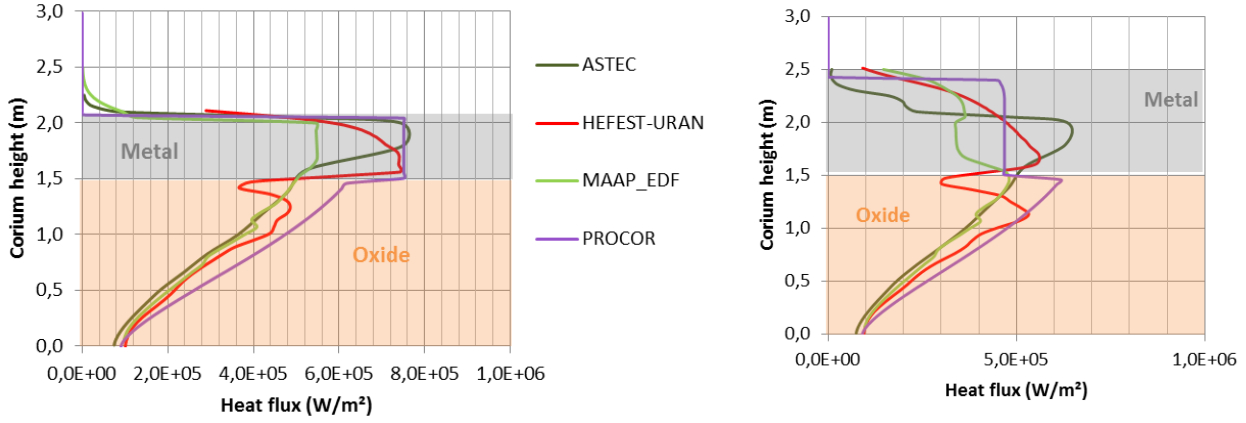

(a) at the time the maximum value is reached (b) at steady state

Figure 5: Heat flux profile at the outer surface of the vessel in benchmark case n°3 where melt thermochemistry and associated transient stratification are not considered - adapted from (Carénini et al. 2019)

[5] Axial conduction was completely discarded in this simulation.

4. Modelling of melt thermochemistry, mass transfer and transient phase spatial distribution

In this Section, we will now discuss the transient stratification modelling present in the four codes when the liquid miscibility gap in the U-O-Zr-steel system is taken into account.

4.1 Thermochemical equilibrium in the liquid miscibility gap

First of all, the different models rely on an evaluation of the two-layer thermochemical equilibrium expected at steady-state. In HEFEST case, through known MASCA results implemented in the THERMOPHASE model (Ozrin et al. 2010). In ASTEC, MAAP_EDF and PROCOR, the Salay-Fichot model (Salay & Fichot, 2005) also based on MASCA results is used.
In the frame of the IVMR project, some developments have been pursued in MAAP_EDF and PROCOR to go further and have a same thermodynamic representation of the corium-steel system throughout all the different models and closures (including, in particular, both thermochemical equilibrium model and enthalpy-temperature relations as a function of the composition for the closure of energy conservation equations). To fulfill this purpose, the construction of a general "Equation-Of-State" (EOS) for in-vessel corium based on a CALPHAD database has been undertaken. In particular, adopting static interpolation strategies, both the liquidus temperature and component phase partitioning (considering metal liquid, oxide liquid and oxide solid phases) were tabulated over the composition space (and temperature for the phase partitioning). Approaches in MAAP_EDF and PROCOR differ significantly - see (R. Le Tellier et al. 2019) for more details – but are based in both cases on phase Gibbs energy models described by the NUCLEA database. Such an interpolation can be used in replacement of the Salay-Fichot model. Figure 6 illustrates the liquid miscibility gap extent in the composition space in both cases: while the Salay-Fichot model is limited to the liquid region (where the temperature dependency is small and neglected), the interpolation approach can be used to describe the system over the whole temperature range. This is a prerequisite to ensure thermodynamic consistency between melt and crust models when the crust is "explicitly" represented as introduced in MAAP_EDF and PROCOR (version 2.4) codes (see §3.3).

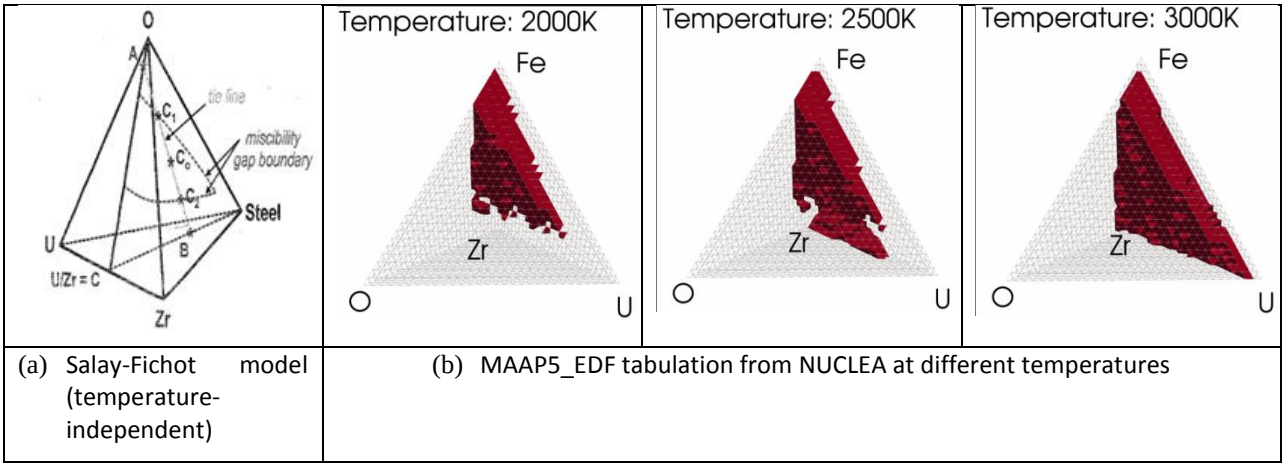

(a) Salay-Fichot model (temperature-independent)

(b) MAAP5_EDF tabulation from NUCLEA at different temperatures

Figure 6: Comparison of the liquid miscibility gap extent in the composition space with the Salay-Fichot model and the NUCLEA database

In addition, to U-O-Zr-steel partitioning between the metallic and oxide phases at equilibrium, decay heat phase distribution has also to be modelled. In PROCOR and MAAP_EDF, a crude assumption is made: the power is distributed proportionally to the U-Zr phase partitioning while in HEFEST and ASTEC, a FPs partitioning based on affinity of species identified from experiments (MASCA in particular) is explicitly evaluated; see (Ozrin et al. 2013) for HEFEST.

4.2 Transient stratification modelling

In HEFEST transient calculations, modification of the stratification occurs over one time-step (while heat generation may relax over a certain time interval). Melt layers inversion is ruled by density ratio criterion (with some tolerance).

On the contrary, in ASTEC, MAAP_EDF and PROCOR, in accordance with the phenomenology discussed in §2, a kinetic model of the inter-layer mass transfer at the interfaces is available and drives the layer inversion process (considering hydrodynamic metal droplets transport as fast in comparison) in such a way that it occurs progressively. These models use a Reynolds' analogy between heat and mass transfers in such a way that available Nusselt correlations (see §3.1) in conjunction with a species diffusion coefficient can be used to evaluate the Sherwood number (and consequently the mass transfer coefficient). In practice, this effective diffusion coefficient value is taken from existing data (range from 10^{-9} to 10^{-8}m²/s) on species self-diffusion coefficients (Alderman et al. 2018).

PROCOR and MAAP_EDF use the same simple model described in (Le Tellier et al. 2015b) that consists in evaluating at each time step the degree of advancement towards global thermochemical equilibrium. It is based on an evolution equation for the Uranium mass fraction in the oxide phase considering a single interface for the exchange with the metal phase (the upper boundary during the heavy metal formation and the lower boundary when stratification inversion is predicted) . This model was "calibrated" against the MASCA-RCW experiment: it is able to correctly predict the heavy metal mass relocated below the oxide with a Uranium effective diffusivity in the range $[3 \times 10^{-9}, 6 \times 10^{-9}]$m^2.s^{-1}.

In ASTEC, a more detailed model based on the physical phenomena analysis performed in (Fichot and Carénini, 2015) has been developed in the frame of IVMR. In particular, thermochemical equilibrium is considered at each interface between oxide and metal layers and not for the total corium pool inventory. At each time step, and for each of the two interfaces, the compositions of the interfacial oxide and metal phases at equilibrium are calculated. Figure 7 and Figure 8 represent the principle of the model with the 2 steps (for the upper and lower interfaces). The example of an initial 2 layer configuration is considered.

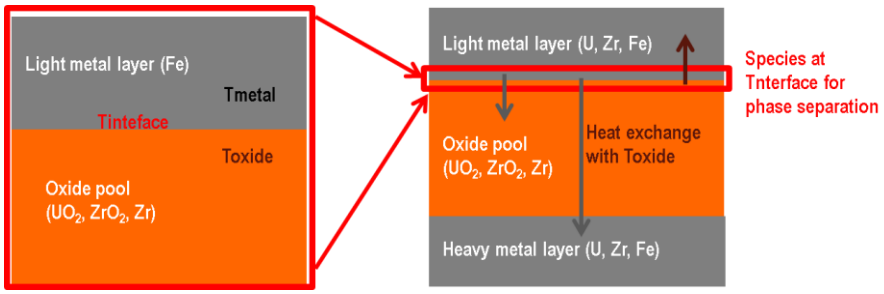

Figure 7: First step of ASTEC stratification model: species interactions and associated mass transfers at the upper interface

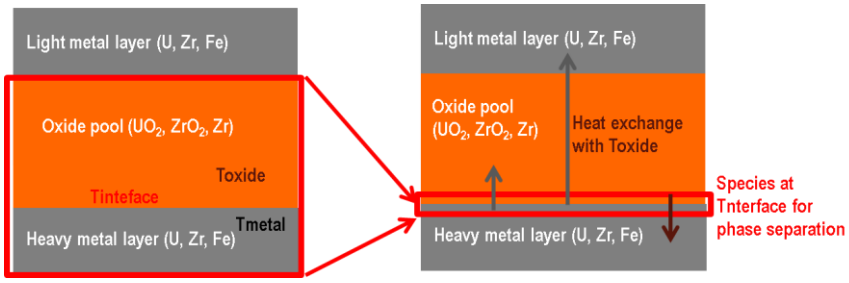

Figure 8: Second step of ASTEC stratification model: species interactions and associated mass transfers at the lower interface

The kinetics of layers stratification is evaluated based on the formulation of the molar flow rate $\alpha_{\mathrm{abl,ox}}$ presented in (Fichot and Carénini, 2015):

$$\alpha_{abl,ox} = \frac{Sh_{up,dw}.D}{L_{up,dw}.L_{int}^{abl,ox}}$$

with

- $Sh_{up,dw}$ the Sherwood number of the oxide layer for upward and downward transfers, depending on the interface considered (respectively with light or heavy metal layer) [-],
- D the species diffusion coefficient in the liquid phases [m²/s],
- $L_{int}^{abl,ox}$ the thickness of the two-phases interaction zone between oxide layer and respectively light metal layer (*abl*) or heavy metal layer (*ox*) [m],
- $L_{up,dw}$ the thickness of the light or heavy metal layers depending on the mass transfers considered [m].

In this model, in addition to the two parameters already exhibited in the MAAP_EDF and PROCOR model (*i.e.* the Nusselt correlation to evaluate the Sherwood number and the species diffusion coefficient), the thickness of the interaction layer is a third parameter which represents the distance for separation of non-miscible phases by gravity.

This parameter depends first on the diffusion process but also on the density difference between the two phases created in the interaction zone which will determine the maximum stable thickness before separation to occur. In ASTEC code, a value of 1mm is considered for the thickness of the interaction layer. However, considering the mass transfers at the interface between the oxide layer and the heavy metal layer, the thickness of the interaction layer is expected to be higher than the one at the top interface, as the density difference between the two phases will be low. Indeed, the heavy metal layer becomes progressively lighter than the oxide layer and a minimal thickness of few centimetres is necessary to initiate destabilization and mass transfers. To consider this effect, a 1cm interaction layer is considered by default in the code, but may be varied by the user for sensitivity studies.

In all codes, thermal inertia associated with stratification inversion ("hot" metal rising to the top of the pool) is taken into account; in MAAP_EDF and ASTEC, a user parameter can be activated to limit this inertia for sensitivity studies.

In both models, the effect of the crust at the light metal/oxide interface is not explicitly modelled. However, in ASTEC model, the effect of interaction between molten steel and the oxide crust on the kinetics of stratification can be considered by choosing the crust thickness for the length of the interaction zone at the top interface and the diffusivity through the crust for the parameter D. In PROCOR and MAAP_EDF model, the impact of the crust can also be taken as a mass transfer barrier for steel coming into interaction with the oxide pool. In MAAP_EDF, a flowrate of the steel depending on its temperature is calculated from a simplified correlation[6] derived from CORDEB/CORDEB2 experiments. In PROCOR, a (user) parameter $\dot{m}_{FE\rightarrow pool}^{\max}$ representing the maximum steel mass flow rate across the crust that can be reached, has been introduced. In this way, the model is able to reproduce the two limiting cases:

- if $\dot{m}_{FE\rightarrow pool}^{max}$ is small (*i.e.* comparable to one obtained in CORDEB-CD1 experiment, the overall stratification kinetics is limited by the mass transfer through the crust;
- if $\dot{m}_{FE\rightarrow pool}^{max}$ is high, the initial behaviour of the model is recovered, the inter-layer kinetics is not affected by the crust.

In addition to its impact on the stratification kinetics, this crust also raises a modelling issue when inversion takes place. While CORDEB/CORDEB2 experimental results show that this crust (with liquid metal above and below) can be stable for a limited period of time, no transient model is available in the codes. In ASTEC (consistently with the overall crust treatment discussed in §3.3), this crust disappears instantaneously in such a way that no light metal layer below the crust is possible. In PROCOR and MAAP_EDF, in addition to ASTEC hypothesis, a four-layer configuration can also be considered assuming that this crust is stable for the remainder of the transient.

[6] This correlation does not account the thickness and chemical composition of the crust.

4.3 Some illustrative results

In order to illustrate the modelling features that have been presented above and the impact of their differences among the four codes, some results of the benchmark cases n°4 and n°5 in (Carénini et al. 2019) are now discussed.

Case n°4 corresponds to the same configuration as case n°3 discussed earlier but melt thermochemistry modelling is activated in the different codes. The thermochemical equilibrium associated to the melt final state corresponds to light metal above oxide. In PROCOR case, a four-layer configuration has been considered in this simulation *i.e.* a light metal layer is formed below the crust during the thermochemical transient. Results of heat flux profiles when the maximum is reached at the outer surface of the vessel are presented in Figure 9 (a). A strong variation of the maximum heat flux is observed in the PROCOR simulation, where the maximum heat flux is reached at the top of the metal layer before injection of molten steel. This high heat flux (up to 5MW/m²) is due to a strong focusing effect occurring in a thin top layer of steel, once the molten steel has interacted with the oxide pool and been transferred below the oxide crust, as shown in Figure 9 (b), with the progressive reduction of top metal layer thickness before molten steel injection and after the stop of injection. In other codes, such assumption regarding the metal relocation below the oxide crust is not made and the oxide crust is supposed to remain at the interface between the oxide and the metal layer, even during chemical interaction and transfer of Zirconium and Uranium in the metal layer. Despite the decrease of the oxide pool mass/height during this interaction, no oxide crust is considered in front of the metal layer (along the vessel wall), assuming that it will lose its integrity. In PROCOR code, this lateral oxide crust in front of the metal layer after its interaction with this oxide leads to significantly decrease the heat flux at this location (below 0.2MW/m²). As a consequence, it is shown that assumptions taken regarding the stability of this oxide crust may have significant impact on maximum heat flux.
It is important to note that, depending on the configuration, it may be conservative or not to consider the stability of the crust. Indeed, in addition to the configuration identified above (risk of strong focusing effect due to the metal layer thinning when it interacts with the oxide below the crust, when the crust is considered as being stable), another risk of high heat flux can be obtained with the assumption of crust instability: metal superheat after stratification inversion and relocation at the top of the pool without being surrounded by the oxide crust. In order to better quantify these potential risks, a deeper understanding of the kinetics of chemical interaction between the oxide crust and the molten metal, as well as its mechanical strength is needed.
In addition, it was noted that the thermochemical interaction between molten steel and oxide is very fast in ASTEC and HEFEST-URAN codes and takes about 5,000s in MAAP_EDF and PROCOR codes. It is also associated to a transfer of fission products in the metallic phase leading to have a fraction of the residual power (15-20%) in the top metal layer.

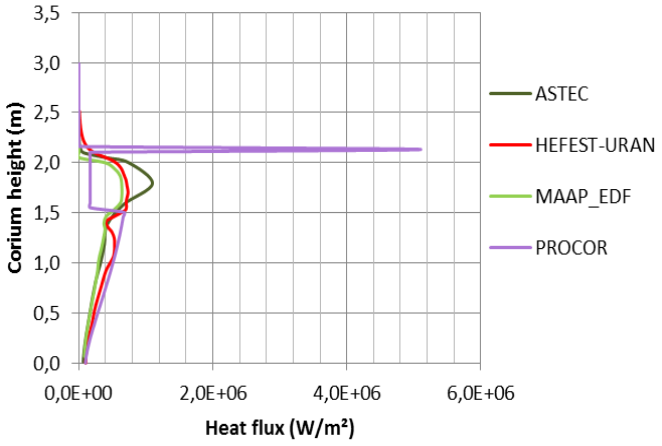

(a) Heat flux profile along the outer vessel wall when

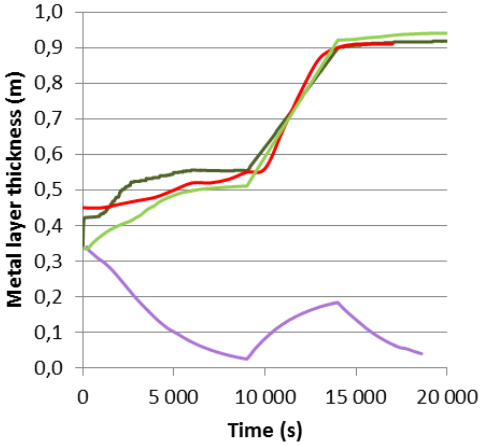

(b) Light metal (above crust) thickness as a

maximum is reached function of time

Figure 9: Results of benchmark case n°4 where melt thermochemistry and associated transient stratification are considered - adapted from (Carénini et al. 2019)

In Case n°5, the Zr oxidation degree of the initial oxide melt was reduced in comparison to the previous cases from 0.63 to 0.3 and the initial mass of steel was reduced from 30t to 10t[7] in such a way that in the first stage of the transient the thermochemical equilibrium corresponds to an heavy metal layer below the oxide. Based on the analysis of the previous case, for the sake of further comparison with the other codes, the oxide crust between the two metal layers is not considered in PROCOR in this case. Results for the maximum heat flux profile reached at the outer surface of the vessel are presented in Figure 10 (a). For each code, the maximum heat flux is multiplied by factor 2 or 3 compared to case without stratification inversion. Looking at the steel evolution in the heavy (Figure 10 (b)) and light (Figure 10 (c)) metal phases, it is shown that the stratification inversion is observed in all simulations, with first the formation of a heavy metal layer and then the progressive decrease of its density up to its relocation to the top of the oxide pool. A significant dispersion of stratification kinetics and threshold for inversion evaluated in the codes is observed. In ASTEC, MAAP_EDF and PROCOR codes, the maximum heat flux is obtained during 3-layers configurations when the top metal layer is thin (due to focusing effect). In HEFEST-URAN code, the maximum heat flux is obtained at stratification inversion due to the superheat of the metal after its relocation through the oxide pool.

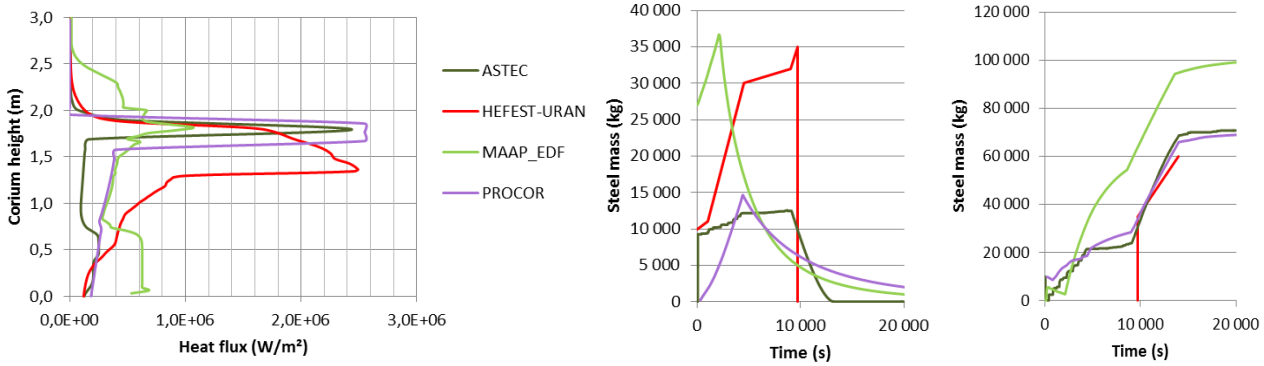

(a) Heat flux profile along the outer vessel wall when maximum is reached

(b) steel mass evolution in the heavy metal layer

(c) steel mass evolution in the top metal layer

Figure 10: Results of benchmark case n°5 where melt thermochemistry and associated transient stratification are considered - adapted from (Carénini et al. 2019)

5. Conclusions

In the context of IVR analysis, salient features of this in-vessel corium transient modelling have been discussed based on a cross-comparison of the models in the ASTEC, HEFEST, MAAP_EDF and PROCOR codes. Results from a recent benchmark exercise carried out in the frame of the IVMR project have been reported to highlight some key issues associated with stratified pool modelling and their impacts on the heat flux imposed to the vessel wall. The four codes are found in fairly good agreement in most cases. The observed differences have been related to the uncertainties on some transient processes and associated diverging modelling hypotheses in the codes. In particular, the impact of the remaining uncertainty on the stratification transients and the stability of the crusts in contact with light metal layer during the stratification inversion transient were shown. Further R&D efforts are needed in order to decrease this uncertainty and meanwhile, the codes should evolve in order to take into account more detailed thermochemical phenomena description. Nevertheless, a quantitative evaluation of IVR with

[7] The additional 20t were considered under the form of an internal structure that is molten during the transient.

transient models can already be done with the current quantification of uncertainties (to be compared with the targeted safety margin).
The reader is referred to a joint paper presented during this seminar (Fichot et al. 2020) for further discussions on the remaining uncertainties in transient modelling.

References

O. L. G Alderman, C. J. Benmore, J. K. R. Weber, L. B. Skinner, A. J. Tamalonis, S. Sendelbach, A. Hebden, M. A. Williamson, "Corium lavas: structure and properties of molten UO2-ZrO2 under meltdown conditions", Scientific Reports, 8, 2434, 2018.

V. I. Almyashev, V. S. Granovsky, V. B. Khabensky, E. V. Krushinov, A. A. Sulatsky, S. A. Vitol, V. V. Gusarov, S. Bechta, M. Barrachin, F. Fichot, P. D. Bottomley, M. Fischer & P. Piluso, "Oxidation effects during corium melt in-vessel retention", Nuclear Engineering and Design, 305, 389-399, 2016.

V. I. Almjashev, V. S. Granovsky, V. B. Khabensky, S. Y. Kotova, E. V. Krushinov, A. A. Sulatsky, S. A. Vitol, V. V. Gusarov, F. Fichot, B. Michel, P. Piluso, R. Le Tellier, M. Fischer, C. Le Guennic & N. Bakouta, "Experimental study of transient phenomena in the three-liquid oxidic-metallic corium pool", Nuclear Engineering and Design, 332, 31-37, 2018.

V. I. Almjashev et al. this seminar.

L. Carénini, F. Fichot & N. Seignour, "Modelling issues related to molten pool behaviour in case of In-Vessel Retention strategy", Annals of Nuclear Energy, 118, 363-374, 2018.

L. Carénini, F. Fichot, N. Bakouta, R. Le Tellier, L. Viot, I. Melnikov, P. Pandazis & A. Filippov, "Main outcomes from the IVR code benchmark performed in the IVMR project", Proc. of the 9th European Review Meeting on Severe Accident Research ERMSAR2019, Prague, Czech Republic, 2019.

P. Chatelard, N. Reinke, S. Arndt, S. Belon, L. Cantrel, L. Carénini, K. Chevalier-Jabet, F. Cousin, J. Eckel, F. Jacq, C. Marchetto, C. Mun & L. Piar, "ASTEC V2 severe accident integral code main features, current V2.0 modelling status, perspectives", Nuclear Engineering and Design, 272, 119-135, 2014.

H. Esmaili & M. Khatib-Rahbar, "Analysis of In-Vessel Retention and Ex-Vessel Fuel Coolant Interaction for AP1000", Technical Report NUREG/CR-6849 ERI/NRC 04-201, U.S. Nuclear Regulatory Commission, Office of Nuclear Regulatory Research, 2004.

Fauske & Associates Inc., "MAAP5 - modular accident analysis program for LWR power plants," in Code Structure and Theory. Electric Power Research Institute, vol. 2, ch. 3, 2008.

F. Fichot, L. Carénini, "Some consequences of material interactions for in-vessel melt retention", Proc. of ICAPP Conference, Nice, France, 2015.

F. Fichot, L. Carénini, M. Sangiorgi, S. Hermsmeyer, A. Miassoedov, S. Bechta, J. Zdarek & D. Guenadou, "Some considerations to improve the methodology to assess In-Vessel Retention strategy for high-power reactors", Annals of Nuclear Energy, 119, 36-45, 2018.

F. Fichot et al. this seminar.

A.S. Filippov, D.D. Kamenskay & E.V. Moiseenko, "Development of the model of heat exchange in a stratified melt in application to severe accident deterministic analysis by SOCRAT/HEFEST code", Bull. Russ. Acad. Sci., Energetics, V. 5, 108-128, 2013 (In Russian).

A.S. Filippov, N.I. Drobyshevsky, D.D. Kamenskay, A.E. Kisselev & E.V. Moiseenko, "End-to-end technology of modeling a melt-structure interaction during IVMR in VVER with HEFEST-URAN toolkit", Proc. of ICONE22, Prague, Czech republic, 2014.

P. Gu, K. Cao & J. Wang, "Research on the Mechanism of Debris Bed Stratification in Vessel Lower Plenum", Proc. of 6th European Review Meeting on Severe Accident Research ERMSAR-2013, Avignon, France, 2013.

R. E. Henry & H. K. Fauske, "External cooling of a reactor vessel under severe accident conditions", Nuclear Engineering and Design, 139, 31-43, 1993.

R. Le Tellier, L. Saas, & F. Payot, "Phenomenological analyses of corium propagation in LWRs: the PROCOR software platform," Proc. of the 7th European Review Meeting on Severe Accident Research ERMSAR-2015, Marseille, France, 2015.

R. Le Tellier, L. Saas & S. Bajard, "Transient Stratification Modelling of a Corium Pool in a LWR Vessel Lower Head Nuclear Engineering and Design", 287, 68-77, 2015.

R. Le Tellier, E. Skrzypek & L. Saas, "On the treatment of plane fusion front in lumped parameter thermal models with convection", Applied Thermal Engineering, 120, 314-326, 2017.

R. Le Tellier, B. Habert, V. Tiwari & N. Bakouta, "Consistent use of CALPHAD data for in-vessel corium pool modeling: some analytical and practical considerations", Proc. of the 9th European Review Meeting on Severe Accident Research ERMSAR2019, Prague, Czech Republic, 2019.

V.D. Ozrin, O.V Tarasov, V. Strizhov & A.S. Filippov, "A model for calculating composition and density of the core melt in the water-moderated water-cooled reactor in case of severe accident", Thermal Engineering, 57, 13, 1099-1111, 2010.

V.D. Ozrin, V.I. Tarasov, A.S. Filippov, E.V. Moiseenko & O.V. Tarasov, "Distribution of fission product residual decay heat in stratified core melt of LWR and its influence on sidewall heat flux", Nuclear Engineering and Design, 261, 107-115, 2013.

M. Peybernes, B. Bigot & R. Le Tellier, "Use of CFD Results to Model Heat Transfer in a Thin Metal Layer", Proc of International Topical Meeting on Advances in Thermal Hydraulics ATH'2020, Palaiseau, France, 2020.

A. Pivano, P. Piluso, N. Chikhi, P. Fouquart, J. Delacroix & R. Le Tellier, "Experiments on interactions of molten steel with suboxidized corium crust for in-vessel melt retention", Nuclear Engineering and Design, 355, 2019.

G. Ratel, F. Deffort, K. Froment, B. Tourniaire & J. M. Seiler, "Considerations on mass transfer kinetics for layer inversion and layer oxidation: from MASCA program to the reactor situation", Proc. of MASCA-2 Seminar, Cadarache, France, 2007.

M. Salay and F. Fichot, "Modeling of metal-oxide corium stratification in the lower plenum of a reactor vessel", Proc. of NURETH-11 Conference, Avignon, France, 2005.

M. Sangiorgi et al. this seminar.

D. F. Tsurikov, V. F. Strizhov, S. V. Bechta, V. N. Zagriazkin & N. P. Kiselev, "Main Results of MASCA1 and 2 Projects", Technical Report, RRC Kurchatov Institute, 2007.

H. Tuomisto & T. G. Theofanous, "A consistent approach to severe accident management", Nuclear Engineering and Design, 148, 171-183, 1994.

H. Tuomisto & B. R. Sehgal, "MASCA results and the case for in vessel melt retention", Proc. of MASCA-2 Seminar, Cadarache, France, 2007.